Available online at www.eccomasproceedia.org
Eccomas Proceedia COMPDYN (2023) 3173-3186

ECCOMAS
Proceedia

COMPDYN 2023
9th ECCOMAS Thematic Conference on
Computational Methods in Structural Dynamics and Earthquake Engineering
M. Papadrakakis, M. Fragiadakis (eds.)
Athens, Greece, 12-14 June 2023

# FRAGILITY CURVES FOR STEEL INDUSTRIAL SILOS ACCOUNTING FOR FILLING LEVEL OF GRANULAR-LIKE MATERIAL

**Mohammad Khalil [1], Sergio Ruggieri [1], Vito Tateo[1], Giuseppina Uva[1]**

[1] Politecnico di Bari, DICATECH Department, Via Orabona4, Bari, Italy

e-mail: {mohammad.khalil, sergio.ruggieri, vito.tateo, giuseppina.uva}@poliba.it

## Abstract

*This study presents an assessment on the seismic fragility of ground-supported steel silos storing solids. As key units in the different industrial sites, storage systems are crucial for the proper and continuous functionality of the relevant industrial operations that can be intended for vital activities such as the food supply. Nevertheless, it is undeniable that storage systems are more vulnerable to seismic events than other units as evidenced in the past. In this context, this work aims to estimate the seismic fragility of ground-supported steel silos, which represent a very common form of storage systems containing granular material. The effect of key factors, such as the silo geometry and the absence/existence of the filling material, which significantly affect the seismic behavior of silos was addressed. In addition, the governing damage patterns is determined. To achieve these goals, two different silos with different distinctive geometries (slender and squat) were investigated considering the empty case and the 90%-filled case. First, a detailed numerical model was built for the investigated cases by using finite element software ABAQUS. After a phase of model validation, the dynamic properties of the silos under investigation were assessed through eigenvalue analysis, while the seismic buckling capacity of the different silos were evaluated through nonlinear static and time-history analysis. Finally, fragility curves of silos were derived by identifying the most critical buckling capacity corresponding to the specific damage patterns, showing the influence of each parameter on the seismic vulnerability and behavior of these kinds of structures.*

**Keywords:** Steel Silos, Granular-like Materials, Nonlinear Time History Analysis, Seismic Fragility.


Peer-review under responsibility of the organizing committee of COMPDYN 2023.
doi: 10.7712/120123.10631.20972

# 1 INTRODUCTION

Storage systems represent vital and critical units in the different industrial sectors. However, in order to ensure a safe and continuous operation of these systems, it is highly important to assess the behavior of the different components of the industrial sites under different sources of risk. Steel silos are storage units that almost no factory is devoid of. They are mainly used to store granular solids covering a wide range of material such as flour, iron ore pellets, cements, chemical materials. Most of these storage systems are steel silos, presenting a circular plan form, although different structural typologies can be adopted. A first classification can be made, distinguishing the ground-supported silos [1,2] and the elevated silos resting on a supporting structure [3,4]. Accounting for the first typology, steel silos are categorized as thin wall shell structures where they are extremely vulnerable to buckling under different load conditions. With this regard, seismic events can provoke disastrous impact on the storage facilities of the industrial systems as evidenced by past significant earthquakes (e.g., 2023 Turkey-Syria Earthquake; 2012 Emilia Earthquake). For instance, Figure 1 shows a recent satellite image of a factory in south of Turkey right after a powerful 7.8 magnitude earthquake struck the area (2023 Turkey-Syria Earthquake). As the image illustrates, the earthquake had the highest destructive impact on the storage systems as the majority of the silos were fully collapsed, although, the other units and ordinary framed industrial structures do not show any collapse. Therefore, it is undeniable that silos are more vulnerable to seismic events than other industrial component. In addition, the loss of containment, which could be encountered in the event of silo failure, can have a propagation effect causing irreparable damage to other units in the industrial sites. Therefore, evaluating the seismic risk of silos is of great importance to avoid the different industrial accident scenarios. The proper functionality of the relevant industrial activities can be guaranteed after an earthquake, as it can be directly connected to logistical activities of rescue operations, food supply, and later to the reconstruction process.

a b

Figure 1: A satellite image of an industrial site following the recent Turkey/Syria earthquake 2023:(a) before; (b)after the earthquake[5].

In the light of the state-of-art reported in Section 2, it is worth mentioning that among the most influencing factors governing the dynamic response of the grain-silo system are: (a) the geometry of the structure; (b) the existence of the ensiled material; (c) the ground motion characteristics. Moreover, as thin wall shell structure, the buckling of the silo wall is the main concern that demands special attention. However, different damage patterns (DPs), or buckling failure modes, might develop in the silo wall under lateral pressure.

In this context, this study investigates the effect of the above-mentioned factors on the behavior and on the failure probability of the grain-silo system under seismic excitation, specifying the most dominant DP. To this aim, two different silos (squat and slender) are investigated under different conditions of functionality (full and empty), and the effect of the ground motion characteristics was implicitly accounted for since different ground motions records were used for performing seismic analysis. First, detailed numerical models were built and validated, after time history (TH) analyses were carried out for each case, finally seismic fragility curves were calculated for each case considering each possible DPs. The results showed in probabilistic term the possibility of each DP to develop, considering the variation of two main parameters: the silo geometry and the effect of the ensiled material existence.

## 2 BACKGROUND

### 2.1 Seismic behavior of ground-supported steel silos

Despite the continuous evolution of the knowledge on the performance-based seismic assessment of different components in the industrial sites such as tanks [6–8], piping systems [9], framed structure [10], elevated silos [3]. The seismic risk assessment of ground-supported steel silos is poorly investigated in the past research. Nevertheless, the principal dynamic behavior and the dynamic characteristics of silos were addressed in the scientific literature since the middle of the last century. In this respect, Lee [11] proposed an analytical model to estimate the portion of mass of the grain which pushes on the silos walls, known as the effective mass, when the system is subjected to dynamic excitation. In this work, a harmonic bass excitation was considered, and the proposed model allowed to observe the variation of the frequencies in the cases of empty and filled conditions. Trahair et al. [12] presented the concept of the additional normal pressure that represent the effect of the seismic response of the stored material on the shell. However, very simple and conservative expressions were introduced to quantify the radial and circumferential pressures applied on the silo wall under horizontal dynamic excitation. Yokota et al. [13] was among the early researchers who employed the finite element techniques to model the cylindrical shell and the ensiled material. This study assumed the coal as ensiled material. In this model, an increasing value in the coal Young's modulus, from the top to the bottom, was considered to account for the confining pressure. The results were compared with the corresponding experimental findings [13] and the natural frequencies calculated on the FE model were 30-40% larger than those obtained based on the experimental test. Shimamoto et al. [14] studied the dynamic response of silo containing coal based on the FE model, using conical shell elements. However, the numerical solution represented by the resonance curves were compared with those obtained based on the tested silo specimens. Rotter and Hull [15] studied the response of circular ground-supported silos (squat) based on elastic FE analysis. The seismic load was represented by quasi-static horizontal body force (uniform horizontal acceleration). In this work, expressions to calculate the stress induced, in the silo wall, by the seismic action were presented. However, this study stated that the membrane stress induced in the wall shell are proportional to R/t ratio and to H/R ratio (R is the radius of the silo, t is the wall thickness and H is the height). Sasaki and Yoshimura [16] presented a numerical model to reproduce a tested scaled silo. In their research, they evaluated the effective mass that pushes on the silo wall under an earthquake. Similarly, Hardin et al. [17] evaluated numerically the seismic response of a large scale steel silos storing wheat. In this study, the grail-silo system modelled by the means of composite shear-beam model accelerated by real earthquake record. The linear elastic behavior was assumed for the silo wall. However, the study recorded the acceleration history, the amplification of the horizontal acceleration, and the stress-strain distribution. Later, Younan and Veletsos [18,19], examined analytically cylindrical silos storing linear viscoelastic solids subjected to earthquake-induced ground motions. The aim of the study was to provide an analytical formulation to describe the seismic response of the filled silo, accounting for the parameters of slenderness ratio and the wall flexibility. Holler and Meskouris [20] characterized the effect of the different component on the silo seismic behavior, mainly accounting for variation of some key parameters, such as the grain-wall interaction, the aspect ratio, the nonlinearity of the granular material, and soil-structure interaction (SSI). The study grounds on the basis of FE numerical modelling considering linear elastic wall behavior. The study concluded that for squat silos, a substantial portion of the ensiled weight does not participate to the horizontal pressures as it is transferred directly to the ground.

Further investigating on the effect of the aspect ratio on the seismic response of flat-bottomed ground-supported silos was presented by Nateghi and Yakhchalian [21]. The study emphasized, based on numerical observations, the influence of the aspect ratio and concluded that assuming a constant value of acceleration distribution along the height of squat silos (adopted by the current European standards EN 1998-4 [22]) leads to conservative design pressures for a squat silo, on the other hand, this assumption is fair for a slender silo. A study presented by Silvestri et al. [23] addressed the matter of the effective mass pushing on the silo wall under seismic action. Grounding on a new physically-based analytical approach, which was later refined by Pieraccini et al. [24], this study emphasized the conservatism of EN 1998-4 [22] provisions with regards to squat silos. In the same framework, a series of shaking table tests was performed by Silvestri et al. [25], on scaled silos made of polycarbonate sheets and containing wheat as ensiled material. This experimental campaign revealed the significant effect of the wall-friction coefficient on the base overturning moment and that is consistent with the analytical approach introduced in [23]. However, this effect is disregarded by the current European provisions of EN 1998-4 [22], which conservatively estimate the base overturning moment. Butenweg et al. [2] further investigated the static equivalent load (adopted by the current European standards EN 1998-4 [22]) by comparing it to more sophisticated approach based on the time history analysis considering nonlinear FE model. The study revealed that considering the equivalent static load, with a simplified linear acceleration along the height, is too conservative for a slender silo. Instead, an acceleration profile determined based on multimodal analysis on a simplified beam is more realistic. Moreover, the study suggested that using the nonlinear numerical modelling leads to more economical design as the equivalent static load approach yields in conservative stress values in case of squat silos and that is in agreement with the statement by [20,23]. Durmus and Livaoglu [26] investigated analytically the seismic behavior of the ground-supported silo based on a simplified model represented by a single degree of freedom flexural cantilever beam with a lumped mass. The study aimed at estimating the dynamic pressure, the base shear force, the fundamental frequency of vibration and the SSI effect. The results obtained by the analytical solution were compared with those obtained based on the numerical simulation. This study stated a good agreement between the results obtained by the two solutions, and it concluded that the effect of SSI can be ignored in practical applications, as it has negligible contribution especially in case of squat silos. Mehretehran and Maleki [27] investigated, by the means of incremental dynamic analysis (IDA), the dynamic buckling behavior of steel silos with a constant thickness. The silos were assumed filled up to 90% of the maximum capacity and the elephant foot buckling was the unique investigated DP. The study estimated the seismic buckling capacity of the relevant silos by the peak ground acceleration (PGA) that initiate the buckling. The main findings of this study indicate that slender silos are more vulnerable to buckling failure while squat silos present a considerably higher resistance under same conditions. Later, the same authors extended their findings to include the stepped wall steel silos under seismic conditions[28]. This study stated that the vertical component of the seismic excitation is of a quite marginal effect. Recently, Silverstri et al. [29] reported a series of shaking table test on full scall flat-bottom steel silo. The considered silo was of corrugated walls and filled with wheat. Basically, this study reported the experimental observation on the static pressure, the dynamic properties, and the dynamic overpressure. On the level of the dynamic behavior, the study found that the fundamental frequency depends on the acceleration and on the compaction of the grains. In addition, the dynamic amplification increases along the height of the silo with maximum value at the top of the ensiled content and the additional normal pressure increases with the depth. Another recent experimental study was presented by Jing et al. [30] based on shaking table test and considering different real and artificial earthquake excitations. The study reported the favorable effect of the existence of the granular material on the energy dispassion of the grain-silo system. In addition, the effect of different filling states on the acceleration vertical profile and on the fundamental frequency of the system was quantified experimentally. For the sake of conciseness, the state-of-art reported above is limited to the ground-supported steel silos which is the most relevant to the subject of this work. Various examples about silos with different typologies, such as elevated silos [3] and reinforced concrete silos [31] can be found in the scientific literature. However, more elaborated state-of-art about the silo structure and their behavior under different conditions is presented in [32,33].

### 2.2 Possible failure modes of ground-supported steel silos

Early investigations on the behavior of storage systems under earthquakes allowed us to gain significant insight into the possible failure modes that can affect the functionality of silos as storage systems. Based on the post-earthquakes site inspections reported in [7,34], a wide variety of possible failure modes and mechanisms of similar structures were reported under earthquake. However, the DPs that can develop in the shell wall, under lateral pressure, are the only connected failure modes to this study. For the case at hand, the considered DPs are: (a) the elastic-plastic buckling known as elephant foot buckling (EFB) [35]; (b) the top-of-wall damage (TWD) which is a possible buckling occurs at the top of the wall [28,34], (c) the elastic buckling occurring near to the middle part of the silo (EB) [7,36].

## 3 CASE STUDY

### 3.1 Silos description

To reflect the variety in the geometry of the silos in the practice, two different silos with different dimensions were considered. A wider set of silos, with similar typology, were studied by Sadowski and Rotter [1] under the condition of discharge loads. The reader may consult the relevant study [1,37] for more details of the conceptual design of the relevant silos. However, the considered silos were chosen to cover slender and squat geometries with properties reported in Table 1. Both considered silos have the same storage capacity (510 m3).

| Typology | Acronym | Height (h) - m | Diameter (D) - m | Thickness (t) - mm | h/D | R/t |
|---|---|---|---|---|---|---|
| Slender | S | 18 | 6.00 | 6 | 3 | 500 |
| Squat | Q | 6.5 | 10.0 | 3 | 0.65 | 1667 |

Table 1: The geometric characteristics of the considered silos.

It is a matter of fact that the existence of the ensiled solids leads to a significant seismic demand. Nevertheless, the existence of the filling material has a favorable impact on the lateral stiffness and imperfection amplitude, and hence on the structure strength. With this regard, it is of high importance to evaluate the influence of the solids' existence on the seismic vulnerability of the silos under investigation and, in this view, the considered silos were studied for the case of empty and 90% filled silo.

### 3.2 Finite element modelling

The three-dimensional EE models of the case study silos were developed using the commercial package ABAQUS (Standard) [38]. Three parts form and assemble the numerical model, that is, the cylindrical steel silo (modelled using the S4R element type) the bulk material stored in the silo (modelled using the C3D8R element), and the concrete base (modelled using the S4R element). This latter was considered as a fully stiff element. Fixed boundary conditions were applied to the steel wall bottom. Giving that the behavior of the shell wall is the main focus of the investigation, the roof structure was ignored in the model. Nevertheless, the effect of the top roof was substituted by considering a rigid body constraint that ties the nodes at the upper edge of the silo wall to a reference point. A careful mesh convergence study was fulfilled for each silo under different analyses. Generally, the mesh considered in the models considers essential considerations. For instance, a greater number of elements should be considered where the stress change rate is high, and less number was used where it is low. For the ensiled material, a higher resolution of mesh was considered at the interface near the wall to ensure a proper developing of the friction interaction between the filling material and the wall. The critical shear stress between the ensiled material and the silo wall was defined according to Coulomb frictional model.

The steel material of the shell wall was assumed as elastic-hardening, with elastic modulus of 210 GPa, yield strength of 275 MPa, ultimate strength of 430 MPa, and strain hardening modulus of 3880 MPa. The considered silos are filled with 'Camacho' wheat [39] with density of 836 kg/m$^3$, angle of internal friction of 22.2°, Young's nodulus of 19.7 MPa, Poisson's ration of 0.37, cohesion of 0.0095 MPa, friction coefficient of 0.19 for steel walls and 0.42 for concrete base. Elastic properties for the filling material were considered to simulate its behavior in the numerical model.

### 3.3 Model validation

Two steps were performed in order to verify the FE model and its static/dynamic outcomes: (a) comparing the static pressure imposed by the filling material on the silo wall with the analytical solution provided by Janssen's theory [40] and modified Reimbert's theory [41]; (b) comparing the dynamic characteristics of the a scaled silo calculated by the numerical modelling with those reported in the literature based on experimental tests [25].

Regarding the first point, the static pressure exerted by the filling material on the silo wall and computed by the numerical analysis were compared with those calculated by the analytical solution provided by [40] for slender silo and [41] for squat silo. Figure 2 depicts the comparison for the considered silos filled up to 90% of the maximum storage capacity, showing a good agreement numerical and analytical solutions.

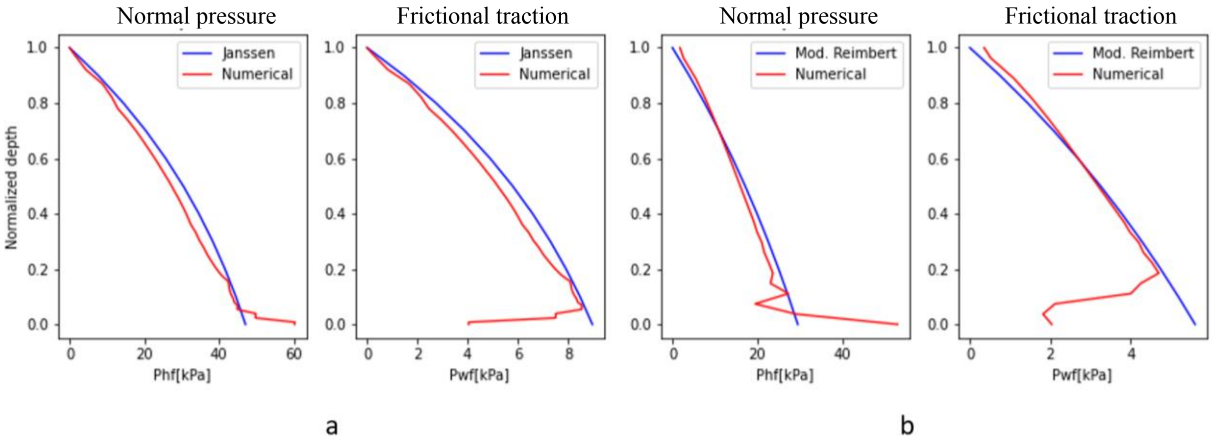


Figure 2: Filling static normal pressures and frictional tractions on the silo walls for the silos Q: (a) 90% filled S-silo; (b) 90% filled Q-silo.

For purpose of verifying the dynamic characteristics yielded from the numerical model, a scaled benchmark silo subjected to shaking table test presented in [25] was modelled. Consequently, eigenvalue analysis was performed and the dynamic characteristics represented by the natural frequency of the dominant vibration modes was calculated and compared with those reported based on the experimental study. The first and second natural frequencies calculated by the FE model were equal to 15.65 Hz and 43.79 Hz, while the ones provided by the experimental test were equal to 12.7-14.1 Hz for the first fundamental vibration mode and 43.9-44.9 Hz for the second one. Also in this case, the comparison between numerical and experimental solutions provided satisfying results.

## 4 SEISMIC ANALYSIS

### 4.1 Frequency analysis

The main dynamic characteristics of the silos under consideration were identified by performing frequency analysis. Fundamental modes of vibration for the silos were observed and the corresponding natural periods were collected. Table 2 reports the periods of vibration for slender and squat cases with empty and 90%-filled condition.

| | 90% | 0% |
|---|---|---|
| S | 0.27 | 0.06 |
| Q | 0.12 | 0.02 |

Table 2: The natural period (in second) of the investigated cases.

### 4.2 Pushover analysis and damage identification

For the purpose of predefining the most vulnerable buckling zones, nonlinear static pushover analysis was performed on the considered silos under investigation. The buckling zones are expected to exhibit severe deformations under lateral loads, and they should be observed when running the dynamic analysis. Nevertheless, the other key reason behind performing pushover analysis is to define the limit of deformation, $EDP_{DP}$, which represent the threshold that state the achievement of the DP, and it was quantified according to a specific engineering demand parameter (EDP) corresponding to each DP. As an instability phenomenon, the shell buckling can be quantified with the displacement magnitude, $\delta$, where this parameter is measured for a control node selected to represent the buckling area under investigation. The parameter $\delta$ was adopted by other studies to quantify the dynamic buckling of silos and similar structures [8,27]. In practice, the buckling can develop in the silo shell body in different positions with different heights. Thus, in order to have a more practical height-unbiased parameter that can neutralize the position of the buckling zone and that account for the silo global behavior, an alternative parameter was used, which is represented by the ratio between the displacement at the monitored point over to the height of the relevant buckling zone, identified with $\theta$. Hence, this unitless parameter can be employed as EDP in the seismic analysis. Figure 3 shows the performance and the deformation shape for the S silo, under a monotonically increased lateral load.

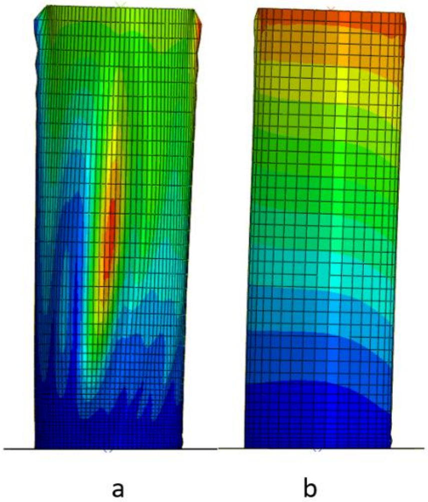


Figure 3: The deformed shape of S silo under lateral static load: (a) the empty case; (b) the 90%-filled case.

The performance of the silo can be interpreted by the behavior of zones prone to buckling corresponding to the distinct DPs. Practically, the behavior of these zones is interpreted by the F-$\theta$ curves, where F represents the global base shear. Consequently, the relevant threshold can be captured as illustrated Figure 4.

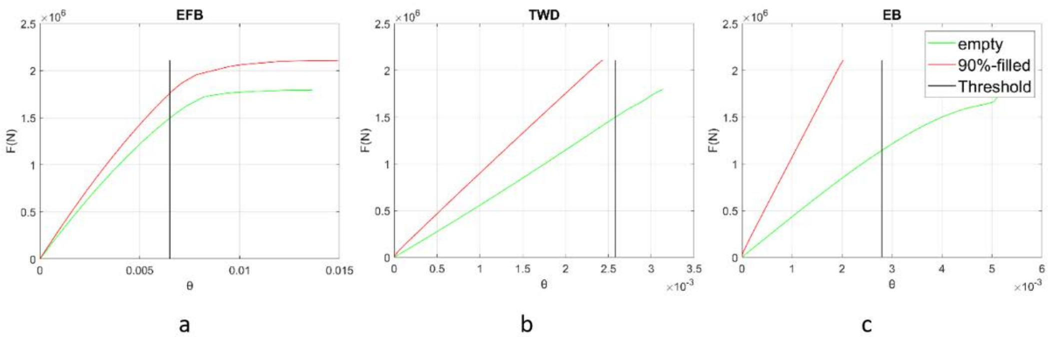


Figure 4: Buckling assessment of the DPs of S silo: (a) EFB; (b) TWD; (c) EB.

### 4.3 Time history analysis

For the purpose of evaluating the dynamic buckling capacity and the variation in the behavior based on the geometry and the absence/presence of the granular material, TH analyses were performed on the silos, accounting for the nonlinearities simulated in the numerical models. For this phase, only half of the system was analyzed since the structure is symmetrical. A damping ratio of 2% was considered for the system. To perform nonlinear TH analyses, the implicit time-integration technique provided by ABAQUS (standard) [38] was used. The model was accelerated by unidirectional ground motions, using 11 natural ground motion records selected according to a high-intensity spectrum (i.e., PGA > 0.25g).

## 5 PROBABLISTIC SEISMIC RESPOSNE ANALYSIS

To estimate the vulnerability of the investigated silos under a seismic action, fragility curves are derived, in order to quantify the probability that a certain DP occurs in the structure for a given seismic intensity measure (IM). To this end, cloud analysis [42] was employed to calculate the fragility of the silo. The results of TH analysis were used to define the EDP-IM pairs that determine the demand-capacity relationship. As IM, the parameter chosen was the spectral acceleration of the first vibration mode, $Sa(T_1)$, in order to well describe the severity of the ground motion on the structure. Nevertheless, PGA could be used, as adopted in [6,27]. To derive the relation between IM and EDP, given the limited number of records, the power law by Cornell was used [43]. Eventually, fragility curves were computed for each case, considering the three possible DPs. Figure 5 presents the fragility curves as output of the analysis. In total, 4 different cases were investigated. As illustrated by the curves in Figure 5, the overall behavior indicates that both silos are most vulnerable to the EFB when the filling material exists, that is, the probability of occurrence of the other expected failure modes (i.e., TWD and EB) is much lesser than that one of EFB, which is the governing DP. However, for empty case the three DPs have roughly similar tendency to develop as graphically demonstrated by the corresponding fragility curves in Figure 5. Values of medians ($\mu$) and dispersions ($\sigma$) were depicted in Table 3, using as subscripts the related DPs.

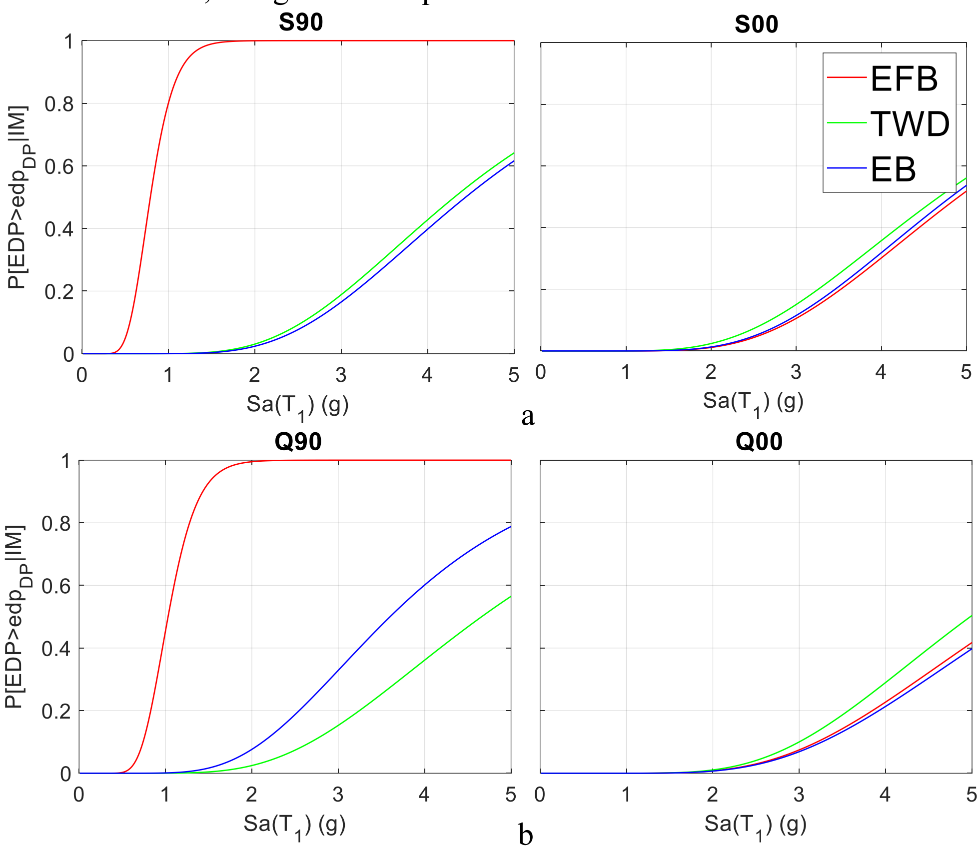


Figure 5. Fragility curves for the investigated silos considering different geometries and filling condition.

| Silo and filling level | | $\mu_{EFB}$ | $\sigma_{EFB}$ | $\mu_{TWD}$ | $\sigma_{TWD}$ | $\mu_{EB}$ | $\sigma_{EB}$ |
|---|---|---|---|---|---|---|---|
| S | 00% | 4.91 | 0.39 | 4.68 | 0.43 | 4.82 | 0.40 |
| | 90% | 0.79 | 0.28 | 4.31 | 0.41 | 4.44 | 0.40 |
| Q | 00% | 5.45 | 0.41 | 4.98 | 0.40 | 5.57 | 0.42 |
| | 90% | 1.03 | 0.26 | 4.66 | 0.43 | 3.60 | 0.41 |

Table 3. Results of fragility curves (μ and $\sigma$) derived for the 4 considered cases.

It is worth noting that the variation in terms of $\mu$ when accounting for 90%-filled or empty cases, reveals that for differences occur for different silo geometry. As a matter of fact, S silo results to be more vulnerable than Q case, looking at the EFB DP ($\mu_{EFB}$ for S equal to 0.79g vs. $\mu_{EFB}$ for Q equal to 1.03). In general, silos with lower aspect ratio performs stronger than those with high aspect ratio and medians corresponding to the governing DPs are higher for squat silos than slender ones, given the same conditions of functionality.

More influent is the role of the ensiled material in the fragility evaluation. Looking at the fragility parameters of the slender silo, the filled silo presents a $\mu_{EFB}$ equal to 0.79g, while the same parameter is equal to 4.91g in the empty case. Still, the relative-high increasing in the median for the empty case indicates very low seismic risk connected to the empty silo, that is, the silo rarely collapses under a natural seismic event for the empty condition. This achievement assume a physical sense, by considering that a very low total mass characterize the empty system, then leading to a low seismic demand.

## 6 CONCLUSIONS

This study presented a numerical evaluation of the seismic fragility for cylindrical ground-supported steel silos storing granular-like material. In detail, the influence of key factors such as the geometry (slender and squat silos) and functionality conditions (fully-filled and empty) were estimated. The governing damage patterns among the possible ones for this kind of structures, i.e. elephant foot buckling, top-wall diamond and elastic buckling in the middle-wall was determined, by computing the seismic fragility for each case.

On the effect of the silo geometry, the results revealed that silos storing solids are most vulnerable to the elephant foot buckling for both slender and squat silos, especially when structures are filled with 90% of the maximum capacity. In addition, both slender and squat silos do not present the tendency to exhibit top-wall damage or diamond elastic middle-wall buckling. In general, the results emphasized that the squat silo performs stronger than the slender one with about 25% higher capacity for the 90%-filled case. About the effect of the ensiled material existence, the results indicated that elephant foot buckling is the governing failure mode for 90%-filled silos while, in case of empty silos, the three investigated damage patterns present comparable probability of occurrence, under very high seismic intensity. On the other hand, empty silos exhibit very high seismic capacity regardless the failure mode and this indicates a very low possibility to fail under ordinary natural seismic events.

Further developments will aim to extend the work on silos to different typologies of silos, storing different class of materials, as well as to refine the numerical models to account other physical factors, e.g., compaction of solid materials during earthquakes action.

## REFERENCES

[1] A.J. Sadowski, J.M. Rotter, Steel silos with different aspect ratios: I — Behaviour under concentric discharge, J Constr Steel Res. 67 (2011) 1537–1544. https://doi.org/10.1016/J.JCSR.2011.03.028.

[2] C. Butenweg, J. Rosin, S. Holler, Analysis of Cylindrical Granular Material Silos under Seismic Excitation, Buildings. 7 (2017) 61. https://doi.org/10.3390/buildings7030061.

[3] A. Kanyilmaz, C.A. Castiglioni, Reducing the seismic vulnerability of existing elevated silos by means of base isolation devices, Eng Struct. 143 (2017) 477–497. https://doi.org/10.1016/j.engstruct.2017.04.032.

[4] R.J. Merino Vela, E. Brunesi, R. Nascimbene, Seismic assessment of an industrial frame-tank system: development of fragility functions, Bulletin of Earthquake Engineering. 17 (2019) 2569–2602. https://doi.org/10.1007/s10518-018-00548-2.

[5] satellite imagery via Google Earth, Maxar, Nurdagi, Turkey @WxNB, (n.d.). https://twitter.com/Maxar/status/1623874874769825793 (accessed March 14, 2023).

[6] M.J. O'Rourke, P. So, Seismic Fragility Curves for On-Grade Steel Tanks, Earthquake Spectra. 16 (2000) 801–815. https://doi.org/10.1193/1.1586140.

[7] E. Brunesi, R. Nascimbene, M. Pagani, D. Beilic, Seismic Performance of Storage Steel Tanks during the May 2012 Emilia, Italy, Earthquakes, Journal of Performance of Constructed Facilities. 29 (2015). https://doi.org/10.1061/(ASCE)CF.1943-5509.0000628.

[8] N. Buratti, M. Tavano, Dynamic buckling and seismic fragility of anchored steel tanks by the added mass method, Earthq Eng Struct Dyn. 43 (2014) 1–21. https://doi.org/10.1002/EQE.2326.

[9] M. Vathi, S.A. Karamanos, I.A. Kapogiannis, K. V. Spiliopoulos, Performance Criteria for Liquid Storage Tanks and Piping Systems Subjected to Seismic Loading, J Press Vessel Technol. 139 (2017). https://doi.org/10.1115/1.4036916.

[10] M. Khalil, Long Span Steel Structures: Structural Typology Optimization and Enhancement- The Conceptual Design of an Aircraft Hangar, in: 2022. https://doi.org/10.11159/iccste22.228.

[11] S.J. Lee, Experimental study of cylindrical silos subject to seismic excitation , Doctoral dissertation, The Ohio State University, 1981.

[12] N.S. Trahair, A. Abel, P. Ansourian, H.M. Irvine, J.M. Rotter, Structural Design of Steel Bins for Bulk Solids, AustralianInstitute of Steel Construction, Sydney, Australia, 1983.

[13] H. Yokota, M. Sugita, I. Mita, Vibration tests and analyses of coal-silo model, in: In Proc., 2nd Int. Conf. on the Design of Silos for Strength and Flow, , Powder Advisory Centre, Stratford-upon-Avon, 1983: pp. 107–116.

[14] A. Shimamoto, M. Kodama, M. Yamamura, Vibration tests for scale model of cylindrical coal storing silo, in: Proceedings of the 8th World Conference on Earthquake Engineering (Vol. 5, San Francisco., 1984: pp. 287–294.

[15] J.M. Rotter, T.S. Hull, Wall loads in squat steel silos during earthquakes, Eng Struct. 11 (1989) 139–147. https://doi.org/10.1016/0141-0296(89)90002-3.

[16] Y. Sasaki, J. Yoshimura, Dynamic discrete modeling and computer simulation of seismic response of concrete stave silos with structural discontinuity. In Earthquake Engineering, in: Proceedings of the Tenth World Conference, Balkema, Rotterdam , 1992: pp. 5065–6070.

[17] B. O. Hardin, R. A. Bucklin, I. J. Ross, Shear-beam Analysis for Seismic Response of Metal Wheat Bins, Transactions of the ASAE. 39 (1996) 677–687. https://doi.org/10.13031/2013.27552.

[18] A.S. Veletsos, A.H. Younan, Dynamics of Solid-Containing Tanks. II: Flexible Tanks, Journal of Structural Engineering. 124 (1998) 62–70. https://doi.org/10.1061/(ASCE)0733-9445(1998)124:1(62).

[19] A.H. Younan, A.S. Veletsos, Dynamics of Solid-Containing Tanks. I: Rigid Tanks, Journal of Structural Engineering. 124 (1998) 52–61. https://doi.org/10.1061/(ASCE)0733-9445(1998)124:1(52).

[20] S. Holler, K. Meskouris, Granular Material Silos under Dynamic Excitation: Numerical Simulation and Experimental Validation, Journal of Structural Engineering. 132 (2006) 1573–1579. https://doi.org/10.1061/(ASCE)0733-9445(2006)132:10(1573).

[21] F. Nateghi, M. Yakhchalian, Seismic behavior of silos with different height to diameter ratios considering granular material-structure interaction, International Journal of Engineering. 25 (2012) 25–35. https://doi.org/10.5829/idosi.ije.2012.25.01b.04.

[22] EN 1998-4, Eurocode 8: Design of Structures for Earthquake Resistance – Part 4: Silos, Tanks and Pipelines, CEN, Brussels, 2006, n.d.

[23] S. Silvestri, G. Gasparini, T. Trombetti, D. Foti, On the evaluation of the horizontal forces produced by grain-like material inside silos during earthquakes, Bulletin of Earthquake Engineering. 10 (2012) 1535–1560. https://doi.org/10.1007/s10518-012-9370-y.

[24] L. Pieraccini, S. Silvestri, T. Trombetti, Refinements to the Silvestri's theory for the evaluation of the seismic actions in flat-bottom silos containing grain-like material, Bulletin of Earthquake Engineering. 13 (2015) 3493–3525. https://doi.org/10.1007/s10518-015-9786-2.

[25] S. Silvestri, S. Ivorra, L. Di Chiacchio, T. Trombetti, D. Foti, G. Gasparini, L. Pieraccini, M. Dietz, C. Taylor, Shaking-table tests of flat-bottom circular silos containing grain-like material, Earthq Eng Struct Dyn. 45 (2016) 69–89. https://doi.org/10.1002/eqe.2617.

[26] A. Durmuş, R. Livaoglu, A simplified 3 D.O.F. model of A FEM model for seismic analysis of a silo containing elastic material accounting for soil–structure interaction, Soil Dynamics and Earthquake Engineering. 77 (2015) 1–14. https://doi.org/10.1016/j.soildyn.2015.04.015.

[27] A.M. Mehretehran, S. Maleki, 3D buckling assessment of cylindrical steel silos of uniform thickness under seismic action, Thin-Walled Structures. 131 (2018) 654–667. https://doi.org/10.1016/J.TWS.2018.07.040.

[28] A.M. Mehretehran, S. Maleki, Seismic response and failure modes of steel silos with isotropic stepped walls: The effect of vertical component of ground motion and comparison of buckling resistances under seismic actions with those under wind or discharge loads, Eng Fail Anal. 120 (2021) 105100. https://doi.org/10.1016/j.engfailanal.2020.105100.

[29] S. Silvestri, S. Mansour, M. Marra, J. Distl, M. Furinghetti, I. Lanese, E. Hernández-Montes, C. Neri, M. Palermo, A. Pavese, E. Rizzo Parisi, A.J. Sadowski, F. Selva, T. Taniguchi, L. Vadrucci, F. Weber, Shaking table tests of a full-scale flat-bottom manufactured steel silo filled with wheat: Main results on the fixed-base configuration, Earthq Eng Struct Dyn. 51 (2022) 169–190. https://doi.org/10.1002/eqe.3561.

[30] H. Jing, H. Chen, J. Yang, P. Li, Shaking table tests on a small-scale steel cylindrical silo model in different filling conditions, Structures. 37 (2022) 698–708. https://doi.org/10.1016/j.istruc.2022.01.026.

[31] F. Nateghi, M. Yakhchalian, Seismic Behavior of Reinforced Concrete Silos Considering Granular Material-Structure Interaction, Procedia Eng. 14 (2011) 3050–3058. https://doi.org/10.1016/j.proeng.2011.07.384.

[32] S. Mansour, S. Silvestri, A.J. Sadowski, The ‘miniature silo’ test: A simple experimental setup to estimate the effective friction coefficient between the granular solid and a horizontally-corrugated cylindrical metal silo wall, Powder Technol. 399 (2022) 117212. https://doi.org/10.1016/j.powtec.2022.117212.

[33] M. Khalil, S. Ruggieri, G. Uva, Assessment of Structural Behavior, Vulnerability, and Risk of Industrial Silos: State-of-the-Art and Recent Research Trends, Applied Sciences (Switzerland). 12 (2022). https://doi.org/10.3390/APP12063006.

[34] P.K. Malhotra, T. Wenk, M. Wieland, Simple Procedure for Seismic Analysis of Liquid-Storage Tanks, Https://Doi.Org/10.2749/101686600780481509. 10 (2018) 197–201. https://doi.org/10.2749/101686600780481509.

[35] J.M. Rotter, Elephant’s foot buckling in pressurised cylindrical shells, Stahlbau. 75 (2006) 742–747. https://doi.org/10.1002/STAB.200610079.

[36] J.C. Virella, L.E. Suárez, L.A. Godoy, A Static Nonlinear Procedure for the Evaluation of the Elastic Buckling of Anchored Steel Tanks Due to Earthquakes, Journal of

Earthquake Engineering. 12 (2008) 999–1022. https://doi.org/10.1080/13632460701672714.

[37] A.J. Sadowski, J.M. Rotter, Steel silos with different aspect ratios: II — behaviour under eccentric discharge, J Constr Steel Res. 67 (2011) 1545–1553. https://doi.org/10.1016/J.JCSR.2011.03.027.

[38] Dassault Systèmes Simulia, Abaqus CAE User's Manual, (2012), (n.d.).

[39] M. Moya, P.J. Aguado, F. Ayuga, Mechanical properties of some granular agricultural materials used in silo design, Int Agrophys. 27 (2013) 181–193. https://doi.org/10.2478/v10247-012-0084-9.

[40] H.A. Janssen, Versuche uber getreidedruck in silozellen, Zeit. D. Ver. Dtsch. Ing. (1895) 1045–1049.

[41] M.L. Reimbert, A.M. Reimbert, Silos : theory and practice, (1976).

[42] P. Bazzurro, C.A. Cornell, N. Shome, J.E. Carballo, Three Proposals for Characterizing MDOF Nonlinear Seismic Response, Journal of Structural Engineering. 124 (1998) 1281–1289. https://doi.org/10.1061/(ASCE)0733-9445(1998)124:11(1281).

[43] C.A. Cornell, F. Jalayer, R.O. Hamburger, D.A. Foutch, Probabilistic Basis for 2000 SAC Federal Emergency Management Agency Steel Moment Frame Guidelines, Journal of Structural Engineering. 128 (2002) 526–533. https://doi.org/10.1061/(ASCE)0733-9445(2002)128:4(526).